# Safety evaluation of mixed traffic flow with truck platoons equipped with (cooperative) adaptive cruise control, stochastic human-driven cars and trucks on port freeways

Chenming Jiang[a,b], Shicong Yin[c], Zhihong Yao[d], Junliang He[a,e] *, Rui Jiang[f], Yu Jiang[b]

[a] China Institute of FTZ Supply Chain, Shanghai Maritime University, Shanghai 201306, China
[b] Management School, Lancaster University, Lancaster LA1 4YW, United Kingdom
[c] Petroleum Business Division, Shanghai Petroleum and Natural Gas Exchange, Shanghai 200120, China
[d] School of Transportation and Logistics, Southwest Jiaotong University, Chengdu, Sichuan 610031, China
[e] Institutes of Logistics Science and Engineering, Shanghai Maritime University, Shanghai 201306, China
[f] School of Systems Science, Beijing Jiaotong University, Beijing 10044, China

* *Corresponding author*. E-mail: jlhe@shmtu.edu.cn

**Abstract**

This study examines the operational safety levels of a novel, complex traffic flow mixed with truck platoons equipped with (cooperative) adaptive cruise control, known as TPs-(C)ACC (referred to as TPs), as well as traditional human-driven cars (HDCs) and trucks (HDTs) in various scenarios on port freeways. The stochastic behavior of human drivers in car-following situations is captured using the stochastic intelligent driver model (SIDM). In contrast, the car-following behaviors of TPs are modeled using the Adaptive Cruise Control (ACC) and Cooperative Adaptive Cruise Control (CACC) models, respectively. Surrogate safety measures (SSMs) are employed to evaluate the safety performance of the mixed traffic flow. The experimental findings demonstrate that, all else being equal, the oscillation of the mixed traffic flow considered in this study diminishes as the penetration rate and lengths of TPs increase, respectively. The safety levels of the mixed traffic flow would be improved with longer TPs but deteriorate with higher total traffic flow rates. For a given CACC intra-platoon headway, larger headways of ACC truck leaders are advantageous to enhancing the safety levels of the mixed traffic flow. However, for TPs with a shorter headway of leading trucks, higher penetrations of TPs with shorter platoon lengths would worsen the safety levels of the mixed traffic flow. When considering a fixed combination of penetration rates, replacing an ACC truck leader with a CACC truck leader improves the safety of the mixed flow, while the incremental effects of lengthening the TPs on enhancing the safety levels diminish. A mixed flow with longer TPs is more susceptible to the stochastic behavior of human drivers.

***Keywords:*** *Safety analysis; Mixed traffic flow; Stochasticity; Trucks platoons equipped with (cooperative) adaptive cruise control; Heterogeneous traffic flow*

# 1 Introduction

Aided by the development of connected and automated technology, Truck Platoons equipped with (Cooperative) Adaptive Cruise Control, i.e., TPs-(C)ACC, allow trucks to drive with virtual connection and communication with each other in a closer inter-vehicle distance. Specifically, a TP-(C)ACC, or a TP for short, refers to a group of container trucks with an ACC truck leader and several CACC truck followers. For simplicity, we will use the terminology of truck platoons (TPs) to refer to TP-(C)ACC in the rest of the paper. The TP has a great potential to increase the capacity of freight roadways (Jo et al., 2019; Bhoopalam et al., 2018; Lioris et al., 2017; Shladover et al., 2015; van Arem et al., 2006), improve traffic stability and safety (Faber et al., 2020; Axelsson, 2016), and reduce fuel consumption and pollutant emissions (Pi et al., 2023; Yao et al., 2021). These benefits of TPs would also be helpful to elevate the levels of intellectualization of the port logistics industry and freight transportation system (Lyu et al., 2022). As a newcomer, the TP has recently joined the traditional traffic flow mixed with conventional human-driven cars (HDCs) and human-driven trucks (HDTs). Scholars evaluated the traffic efficiency and safety of TPs by varying platoon characteristics and tested their proposed models on the A15 motorway near the port of Rotterdam, Netherlands (Faber et al., 2020). While in China, as illustrated in Fig. 1, the TP program has been undertaken by Shanghai International Port (Group) Co., Ltd. (SIPG), Shanghai Automotive Industry Corporation (SAIC), and China Mobile Limited since the year 2020. This program has been continuously tested in traffic flow mixed with HDCs and HDTs on the freeways of the Donghai Bridge connecting the Shanghai Yangshan Deep-Water Port to the mainland of Shanghai, China, since December 2022.

Then, the operation safety of the new-fashioned, mixed traffic flow would be one of the primary issues for the authority to follow. Concerns about the safety of the TP-related complex traffic flow have recently gained more and more attention (Ma et al., 2023; Faber et al., 2020; van Nunen et al., 2017). However, most studies either focus on the safety of 100% truck platooning (van Nunen et al., 2017) or take into account the safety of mixed traffic flows involving only HDCs and TPs (Deng, 2016; Ramezani et al., 2018; Yang et al., 2019; Faber et al., 2020), which overlook the indigenous but indispensable component on port freeways, i.e., the HDTs.

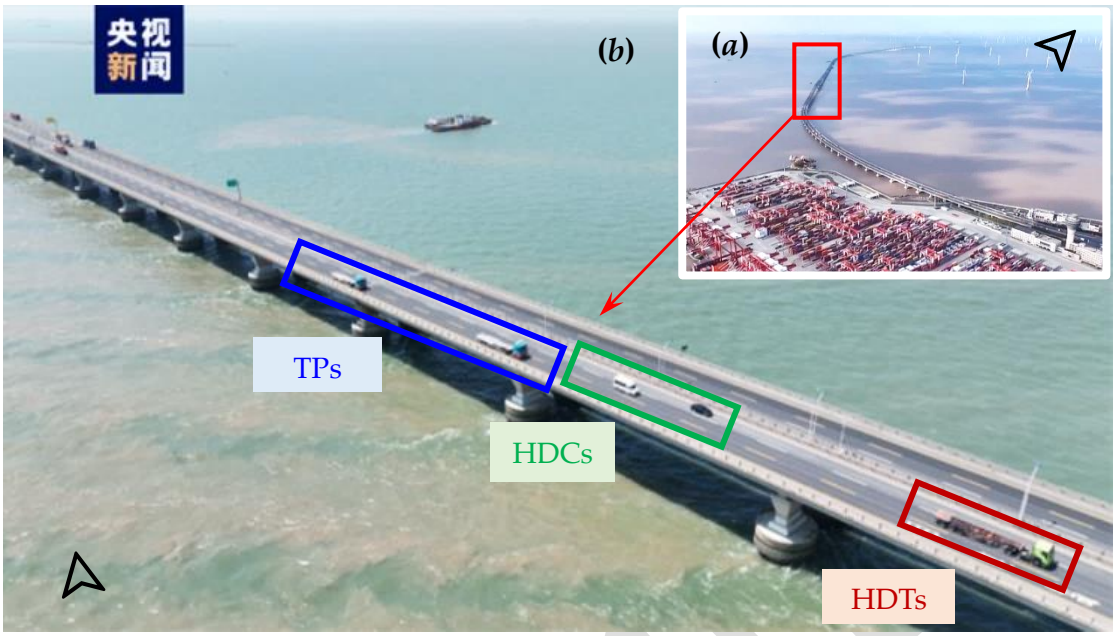


**Fig. 1** The scenario of the coastal traffic flow mixed with TPs, HDCs, and HDTs on the freeways of Yangshan Deep-Water Port, Shanghai, China. Sources of the base maps: (a)[1] and (b)[2]

Besides, quite a few studies have recently demonstrated that stochastic factors are responsible for the traffic oscillations and instability of the traffic flow (Bouadi et al., 2024; Bouadi et al., 2022; Wang et al., 2020; Jiang et al., 2018; Tian et al., 2019), which further harms the safety and results in collisions. The stochastic nature of human drivers can derive from different aspects, e.g., heterogeneous real-time judgment and reactions on the same driving scenarios, temporal variations of the driver's habits/behavior, or the true randomness of some unconscious decisions of the drivers (Bouadi et al., 2022). However, the stochasticity of human drivers has not aroused enough attention in the existing studies on the safety analysis of mixed traffic flow with human-driven vehicles (HDVs) and connected and automated vehicles (CAVs). Neglecting stochasticity also makes it challenging to meet the practical demand in operation safety when TPs are implemented in related industry scenarios like port logistics.

To close the gaps, this paper aims to evaluate the safety of the mixed traffic flow composed of three types of vehicles, i.e., TPs, HDCs, and HDTs, considering the effects of human drivers' stochasticity. Safety performance levels of the mixed traffic flow would be evaluated by conducting numerical simulation modeling and sensitivity analysis. Accordingly, this study contributes to the literature from the following three facets: (1) as far as the authors know, this study would be the first attempt to evaluate the safety issue of

[1] https://content-static.cctvnews.cctv.com/snow-book/video.html?t=1640389774656&toc_style_id=video_default&share_to=wechat&track_id=2F8013CA-8D0F-4E80-BF67-18D2CE6F383D_662086829035&item_id=2309057031324917814

[2] https://www.utopilot.com.cn/news/136.html

the novel, complex traffic flow mixed with tripartite components, i.e., HDCs, HDTs, and *scheduled* TPs against the backdrop of port logistics. (2) The stochastic effects of human-driven vehicles (i.e., HDCs and HDTs) on the safety of the mixed traffic flow were investigated by utilizing the stochastic IDM (SIDM) recently proposed by Bouadi et al. (2022). (3) Compared to the traditional CACC model utilized by most studies, this work adopted a more effective model considering the transmission effects of acceleration of the preceding truck on the CACC followers in a TP. Through numerical simulation experiments, this paper examines a wide range of factors that may impact the safety performance of the complex mixed traffic flow (such as TP lengths, the mixed flow rates, TP headway combinations, types of TP leaders, and stochasticity strengths).

The remainder of this paper is structured as follows. Section 2 reviews studies on TP modeling, car-following stochasticity, and safety analysis of CAV-related mixed traffic flow. The methodological underpinnings utilized in this work are presented in Section 3, which includes the configuration patterns, car-following models, and safety analysis measures. The details of simulation-based safety analysis, including experimental design, the analysis of experimental results, and sensitivity, are investigated in Section 4. Section 5 concludes this study and discusses future research directions.

# 2 Literature review

## 2.1 Truck platoons equipped with (cooperative) adaptive cruise control

As intelligent driving and vehicle-to-vehicle (V2V) communication technologies have advanced, CAV has drawn more and more attention in recent years (Jiang e al., 2020). The control patterns of CAVs are generally divided into two categories, i.e., adaptive cruise control (ACC)[3] and cooperative adaptive cruise control (CACC)[4] (Shladover et al., 2015). The PATH[5] at the University of California at Berkeley establishes ACC/CACC truck-following models based on long-term field vehicle data. It proposes expected headways for safe ACC/CACC truck platooning (Shladover et al., 2018). In addition to comparing the CACC with truck platooning, Nowakowski et al. (2016) provided a more precise description of the CACC operating functions for trucks. Ramezani et al. (2018) integrated the control models of CACC/ACC trucks using the experimental data. They demonstrated that CACC trucks have an advantage over conventional ones in increasing vehicle miles traveled,

[3] Adaptive Cruise Control (ACC) is an advanced driver assistance system (ADAS) that uses radar or laser sensors to automatically adjust the speed of a vehicle to maintain a safe distance from the vehicle in front.

[4] Cooperative Adaptive Cruise Control (CACC) is a more advanced version of ADAS that enables vehicles to communicate with each other to improve traffic flow and safety, and reduce congestion on highways. In CACC, vehicles exchange information about their position, speed, and acceleration using V2V communication.

[5] Partners for Advanced Transportation Technology Lab at the UC Berkeley.

average speed, and flow rate. Moreover, the operation of passenger cars was not significantly harmed by the presence of CACC trucks. This study considers *scheduled platooning* to be the type of TP planning[6]. Also known as off-line or static planning, *scheduled platooning* is a plan made in advance without modifications *en route* (Bhoopalam et al., 2018), widespread in the early stages of TP development.

The connected and automated technology enables trucks to form TPs with a minor headway in freight logistics. Closer following distance in a TP increases the roadway capacity and reduces fuel consumption by lowering wind resistance. Test results show that a platoon's leading vehicle can save up to 6% of its fuel while the following vehicles can save up to 10% (Alam et al., 2015; Lammert et al., 2014), which benefits individual truck operators as well as the whole trucking industry. As a result, TP has recently sparked a lot of interest in both business and academia. The car-following behavior (Ramezani et al., 2018), the control strategy (Chen et al., 2018) of TPs, and the impact of TPs on traffic flow (Calvert et al., 2019) were also investigated by previous studies. The possible influence of TP on traffic flow performance was empirically and quantitatively analyzed by Calvert et al. (2019). The findings revealed that the TP has a minor negative impact on unsaturated traffic capacity but a more significant negative impact on saturated flow. Bhoopalam et al. (2018) analyzed relevant operations research models and a framework for classifying numerous new transportation planning issues emerging in the TP. Results of simulation experiments conducted on a 3.5 km long two-lane roadway by Deng (2016) show that as the TP market penetration rises, the average traffic volume dramatically increases while the spatial average speed declines. The findings of simulation experiments conducted by Wang et al. (2019) examined the effects of truck platooning on freeway operations. They showed that the TP raised the maximum flow by 19% under congested conditions but had no appreciable impact under free flow conditions.

### 2.2 Stochasticity of the car-following behavior

Stochastic phenomena are one of the most common objective phenomena in the real world, and scholars generally describe them using stochastic approaches. The stochastic approach is a probabilistic and random-based analytical approach used for addressing complex problems or simulating phenomena with uncertainty (Graham and Talay, 2013). It primarily includes Monte Carlo simulation (Rubinstein and Kroese, 2016), Markov Chain Monte Carlo (Brooks et al., 2011), stochastic optimization (Schneider and Kirkpatrick, 2007), and stochastic differential equations (Protter, 2005), etc. The stochastic approach finds wide applications across various academic disciplines, including mathematics, statistics, physics, economics, etc. The advantages of the stochastic approach lie in its ability to simulate and

[6] For simplification, we continue to use TP to stand for the *scheduled TP* in the remaining of this paper.

analyze uncertainty and randomness in the real world, often offering more flexibility compared to deterministic methods (Kalos and Whitlock, 2009). However, the disadvantages of this approach involve that it typically requires substantial computational resources and time, especially when dealing with large-scale systems or complex models (Binder et al., 1992). Additionally, the results obtained from the stochastic approach are generally based on probability and statistical inference, which may introduce certain levels of uncertainty and error.

In transportation, the car-following behavior of human drivers is known as the fundamental longitudinal motion in the traffic flow, usually formulated as car-following models. Dominant car-following models include the full velocity difference model (Jiang et al., 2001) and the intelligent driver model (IDM, Treiber et al., 2000), which have been widely acknowledged to depict the HDVs' car-following mechanism in the traffic flow. The IDM regards a vehicle's car-following movement as driven by a resultant force composed of a driver's pursuit of his desired speed and the constrained resistance formed by the leading vehicle ahead of the ego vehicle (Treiber et al., 2000).

As the effects of stochasticity on the stability of traffic flow have recently raised concerns in academia, it is widely believed that the presence of stochastic factors should be explicitly considered for a better prediction of traffic instability (Jiang et al., 2015, 2018; Tian et al., 2019). Xu and Laval (2019) investigated a simplified traffic flow model in which stochasticity is proportional to the velocity. Ngoduy et al. (2019) conducted a string stability analysis of a stochastic optimal velocity model by introducing the Wiener process. Both of them found that stochasticity induces traffic instability and deteriorates traffic performance.

**2.3 Safety analysis of the mixed traffic flow**

The instability resulting from stochasticity is believed to be highly related to traffic safety (Yao et al., 2020; Yao et al., 2019). Many studies have been conducted on traffic flow safety mixed with CAVs and HDVs. In long traffic platoons, that oscillation amplitude tends to exacerbate quickly. It forces ACC vehicles further upstream to apply strong braking followed by a strong acceleration, thus causing significant safety risks (Li et al., 2021). Given that conventional safety measures like crash frequency and injury severities are sometimes unavailable (Jiang et al., 2021; Wang et al., 2021; Jiang et al., 2016; Xing et al., 2014), surrogate safety measures (SSMs) are alternatively utilized to describe and assess the safety of traffic flow (Dai et al., 2023; Tu et al., 2019; Jiang et al., 2023). Time-to-collision (TTC, Hayward, 1972), and two TTC-based derivatives SSMs, i.e., time-exposed TTC (i.e., TET) and time-integrated TTC (i.e., TIT) (Minderhoud and Bovy, 2001), are among the most widely used SSMs to evaluate the safety performance or the collision risk of traffic flow. Li et al. (2017a, 2017b) utilized TET and TIT to investigate the effects of ACC and CACC-equipped vehicles on the risk of rear-end collisions under various CAV penetration rates. Simulation results show that the risk of rear-end collisions between CAVs on the freeway can be significantly

decreased with the increased penetration rate of CACC vehicles. Considering the degradation of CACC vehicles into ACC ones due to communication failures, Yao et al. (2020) explored the stability and safety of a mixed traffic flow composed of CACC cars, ACC cars, and HDCs. The findings show that more CACC cars significantly reduce the crash risks when the penetration rate of CACC cars hits 50%. Mahdinia et al. (2020) studied the impacts of automated and cooperative systems in mixed traffic containing conventional, ACC, and CACC vehicles. They learned that the use of a CACC system in a five-vehicle platoon significantly reduces the risk of rear-end collision, thus improving safety. Faber et al. (2020) utilized a microscopic emulator *OpenTrafficSim* to simulate the TP's collision-free and smooth driving behavior in the traffic flow mixed with cars and truck platoons. Regarding platooning, Yao et al. (2023) recently discovered that the maximum platoon size of CAVs increases the safety risk of the mixed traffic flow. The presence of HDTs harms the formation of truck platooning and deteriorates the longitudinal safety levels of the mixed flow (Zhang et al., 2022). Similarly, the above studies have not investigated the safety performance of complex traffic flow mixed with HDCs, HDTs, and TPs. Bai et al. (2024) investigated heterogeneous traffic flow with or without an ACC system for the pair of a front truck and a rear passenger car. They found that as more ACC vehicles enter the market, the likelihood of collisions between the front truck and rear car drops, and the ACC rear car exhibits a lower probability of conflicts than the conventional vehicles.

In summary, many studies have conducted safety analyses of traffic flow mixed with CAVs and HDVs. Still, the effects of stochasticity on the safety of mixed traffic flow have recently been ascendant. Table 1 provides an overview of the pertinent studies in which HDVs refer to the HDCs and HDTs. However, two aspects have received relatively scant attention in prior studies: (1) Little attention has been paid to the safety mechanism of TP operating in complicated traffic flows mixed with HDCs and HDTs; (2) there also lacks sufficient consideration of the human drivers' stochasticity on the safety of the mixed traffic flow. To fill these gaps, this study aims to evaluate the safety of the flow mixed with HDCs, HDTs, and TPs considering human drivers' car-following stochasticity.

**Table 1** Summary of the existing studies on the safety analysis of the mixed traffic flow with HDVs and CAVs.

| Author, Year | HDV types | | CAV types | | Stochasticity | Safety |
|---|---|---|---|---|---|---|
| | Passenger car (HDC) | Truck (HDT) | Passenger car (CAV) | Truck platoon (TP) | | |
| Deng (2016) | ✓ | ✗ | ✗ | ✓ | ✗ | ✓ |
| Li et al. (2017b) | ✓ | ✗ | ✓ | ✗ | ✗ | ✓ |
| van Nunen et al. (2017) | ✗ | ✗ | ✗ | ✓ | ✗ | ✓ |
| Ramezani et al. (2018) | ✓ | ✗ | ✗ | ✓ | ✗ | ✗ |
| Calvert et al. (2019) | ✓ | ✓ | ✗ | ✓ | ✗ | ✗ |
| Yang et al. (2019) | ✓ | ✗ | ✗ | ✓ | ✗ | ✓ |
| Faber et al. (2020) | ✓ | ✗ | ✗ | ✓ | ✗ | ✓ |
| Mahdinia et al. (2020) | ✓ | ✗ | ✓ | ✗ | ✗ | ✓ |
| Yao et al. (2020) | ✓ | ✗ | ✓ | ✗ | ✗ | ✓ |
| Yao et al. (2022) | ✓ | ✗ | ✓ | ✗ | ✗ | ✗ |
| Zhang et al. (2020) | ✓ | ✓ | ✓ | ✗ | ✗ | ✓ |
| Zhang et al. (2022) | ✓ | ✓ | ✓ | ✗ | ✗ | ✗ |
| Jiang et al. (2023) | ✓ | ✗ | ✓ | ✗ | ✗ | ✓ |
| Bai et al. (2024) | ✓ | ✓ | ✗ | ✗ | ✗ | ✓ |
| **This study** | ✓ | ✓ | ✗ | ✓ | ✓ | ✓ |

# 3 Methodology

## 3.1 Compositions of the mixed traffic flow

This study utilizes numerical simulation-based models to validate the safety performance of the novel complex traffic flow mixed with traditional HDCs, HDTs, and TPs on container port freeways. More specifically, as shown in Fig. 2, the mixed traffic flow considered in this study is composed of three types (four sub-types) of vehicles, i.e., (1) HDCs (the red car), (2) HDTs (the red truck), and TP (the blue ACC leader and green CACC followers).

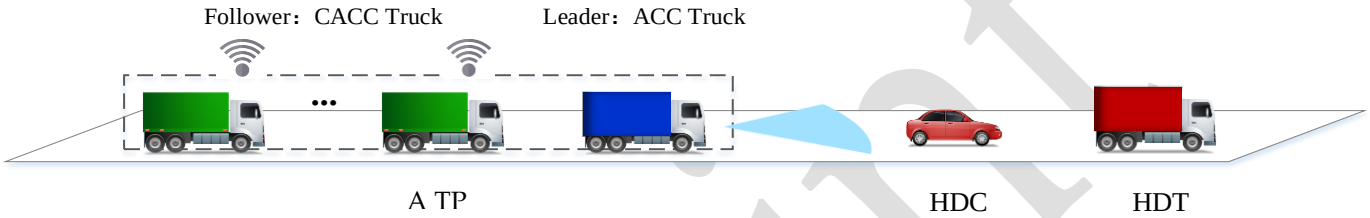


**Fig. 2** One of the scenarios regarding the composition of the mixed traffic flow considered in this study.

As shown in Fig. 2, a TP herein consists of a platoon leader and several followers. They are assumed that the leader of a TP is ACC-based truck which degrades from a CACC truck (i.e., the blue truck in Fig. 2), which means that the leader cannot communicate with the vehicle in front no matter what kind of the anterior vehicle is (Li et al., 2017b) but still can transmit its kinematic parameters (e.g., the acceleration, location, and speed, etc.) to its adjacent follower (Yao et al., 2022). In contrast, the followers (i.e., the green trucks) within a TP can communicate with adjacent teammates via a CACC technique. A TP usually comprises no more than ten trucks (Lee et al., 2020) and can approach up to 100 meters due to the massive bulks, extended body sizes, and larger truck headways than cars. We define the platoon length $L$ of all scheduled TPs as the total number of trucks included in a platoon, which is reasonably assumed to be two to five. In other words, each TP contains one ACC leader and one to four CACC followers.

Assume there are $n$ vehicles in the novel mixed traffic flow, where the penetration rates (%) of HDCs, HDTs, and TPs are denoted as $P_{HDC}$, $P_{HDT}$, and $P_{TP}$, respectively. Let $\mathbf{P}=\{P_{HDC}, P_{HDT}, P_{TP}\}$ represent a specific mixed traffic flow composition scheme in this study. Then, Eq. (1) is satisfied, and the number of all four sub-types of vehicles in the traffic flow can be shown in Eq. (2):

$$P_{HDC} + P_{HDT} + P_{TP} = 1 \tag{1}$$

$$\begin{cases} N_{HDC} = QP_{HDC} \\ N_{HDT} = QP_{HDT} \\ N_{T-ACC} = \dfrac{QP_{TP}}{L} \\ N_{T-CACC} = \dfrac{(L-1)QP_{TP}}{L} \end{cases} \tag{2}$$

in which $N_{HDC}$, $N_{HDT}$, $N_{T\text{-}ACC}$, and $N_{T\text{-}CACC}$ denote the number of HDCs, HDTs, and leading trucks with ACC, and following trucks with CACC in a TP, respectively. $N_{T\text{-}ACC}$ ($L$) is a monotonically decreasing function of the platoon length $L$, while $N_{T\text{-}CACC}$ ($L$) is a monotonically increasing function of $L$. Therefore, other things being equal (especially for a given composition scheme **P**), a particular mixed flow with shorter TPs (i.e., a smaller $L$) would result in more ACC trucks (i.e., a larger $N_{T\text{-}ACC}$) but fewer CACC trucks. According to Eqs. (1) and (2), the number of the four sub-types of vehicles meets the quantitative relationship shown in Eq. (3).

$$N_{HDC} + N_{HDT} + N_{T-ACC} + N_{T-CACC} = Q \tag{3}$$

### 3.2 Car-following models of four vehicle types

*3.2.1 Car-following stochasticity of human-driven vehicles (HDCs and HDTs)*

The IDM developed by Treiber et al. (2000) is a widely used model to simulate a skilled driver's car-following practices, as it formulates a vehicle's acceleration and deceleration changes smoothly without repeated fluctuations (Yu et al., 2021). To be closer to reality, this study considers the stochasticity of the car-following behaviors of HDVs (Bouadi et al., 2022). Based on the IDM, the acceleration rate $a_n^{SIDM}(t)$ of the ego vehicle $n$ at time $t$ in the stochastic IDM (SIDM) considered in this work reads in Eq. (4) and $s^*$ denotes the desired gap given by Eq. (5):

$$a_n^{SIDM}(t) = a[1-(\frac{v_n(t)}{v_f})^4 - (\frac{s^*(v_n(t),\Delta v(t))}{s_n(t)})^2] + \sigma\sqrt{v_n(t)}dW_n \tag{4}$$

$$s^*(v_n,\Delta v) = s_0 + v_n(t)T + \frac{v_n(t)\Delta v(t)}{2\sqrt{ab}}, \tag{5}$$

where the first term of the right side of Eq. (4) denotes the deterministic part as in the standard IDM, while the second term indicates the stochastic component in SIDM. $a$ and $b$ are the maximum acceleration and the comfort deceleration of the ego vehicle, respectively. $v_n(t)$ is the instantaneous speed of the ego vehicle $n$ at time $t$. $v_f$ is the maximal speed in free-flow traffic conditions; $s_n(t) = x_{n-1}(t) - x_n(t) - l$ is the distance between the head of the ego vehicle $n$ and the rear bumper of the leading vehicle $n$-1, and $l$ is the length of the leading vehicle $n$-1. Besides, $\sigma$ is a positive dissipation parameter describing the

stochasticity strength and $dW_n$ denotes the Wiener process (Ngoduy et al., 2019; Bouadi et al., 2022). The dependency on velocity in the second term of the right side of Eq. (4) and the normal distribution (generated by the Wiener process) align with empirical observations. When the velocity tends to zero, the term $\sqrt{v_n(t)}$ will also tend to zero (Bouadi et al., 2022). Conversely, the standard deviation term will be maximal when the velocity tends to be maximal. $s_0$ in Eq. (5) is the minimum safety distance at a quiescent state, $T$ is the safe headway, $\Delta v(t) = v_n(t) - v_{n-1}(t)$ is the speed difference between the leader *n*-1 and the ego vehicle *n* at time *t*.

*3.2.2 ACC and CACC trucks in TPs*

Ramezani et al. (2018) calibrated the parameters of the car-following model of the CATs in a TP in the PATH laboratory. Shladover et al. (2018) reported the acceptance rates of different headways of CATs through field tests. The available time gap of CACC trucks is one of the crucial parameters to indicate the desired following headways, whose values are generally set as 0.6 ~ 1.8s. In contrast, the available time gap was set to be 2.0 s in the middle range of commercially available ACC trucks (Shladover et al., 2018). This paper describes the car-following behaviors of the leading and following trucks in a TP by the ACC and CACC models, respectively.

*(1) The ACC model*

The acceleration rate $a_n^{ACC}(t)$ of the ego vehicle *n* at time *t* in the ACC model (Milanes and Shladover, 2014) is formulated in Eqs. (6) and (7):

$$a_n^{ACC}(t) = k_1 e_n(t) + k_2 \Delta v_n(t) \tag{6}$$

$$e_n(t) = \Delta x_n(t) - l - s_0 - t_a v_n(t) \tag{7}$$

where $k_1$ and $k_2$ are the control parameters. $\Delta v_n(t)$ is as defined in Eq. (5); *e* is the error between the actual and expected gap distance. $\Delta x_n(t) - l - s_0$ is the actual clearance gap, in which $\Delta x_n(t) = x_{n-1}(t) - x_n(t)$ is the space headway between the ego ACC truck *n* and the preceding vehicle *n*-1 (a car or truck) at time *t*. $t_a$ is the expected time headway. $l$ and $s_0$ are as previously defined. $a_n^{ACC}(t)$ can be further written as

$$a_n^{ACC}(t) = k_1 \left( \Delta x_n(t) - l - s_0 - t_a v_n(t) \right) + k_2 \Delta v_n(t) \tag{8}$$

*(2) The CACC model*

The CACC model (Milanes and Shladover, 2014) can be formulated as follows in Eqs. (9) and (10):

$$v_n(t + \Delta t) = v_n(t) + k_p e_n(t) + k_d \dot{e}_n(t) \tag{9}$$

$$e_n(t) = \Delta x_n(t) - l - s_0 - t_c v_n(t) \tag{10}$$

where $v_n(t + \Delta t)$ and $v_n(t)$ are the speeds of the current CACC truck *n* at time *t*+$\Delta t$ and

previous time $t$, respectively. $\Delta t$ is the iteration time step. $k_p$ and $k_d$ are the model control parameters, respectively. $e_n(t)$ is the gap error between the actual gap distance and the expected gap distance of CACC truck $n$ at time $t$. $\Delta x_n(t) = x_{n-1}(t) - x_n(t)$ in Eq. (10) is the gap headway between two contiguous CACC trucks in a TP. $l$ and $s_0$ are as previously defined. $t_c$ is the expected headway of the CACC followers in a TP. $\dot{e}_n(t)$ is the derivative form of $e_n$, as shown in Eq. (11):

$$\dot{e}_n(t) = \Delta v_n(t) - t_c a_{n,0}^{CACC}(t) \tag{11}$$

where $\Delta v_n(t)$ is the speed deviation between two contiguous trucks $n$ and $n$-1 in a TP at time $t$; $a_{n,0}^{CACC}(t)$ is the acceleration rate of the ego CACC truck $n$ at time $t$.

So, a classical CACC model with a constant-time headway and relative-speed can be further obtained as shown in Eq. (12) (Zhang et al., 2024; VanderWerf et al., 2001),

$$a_{n,0}^{CACC}(t) = k_p\left(\Delta x_n(t) - l - s_0 - t_c v_n(t)\right) + k_d \Delta v_n(t) \tag{12}$$

On this basis, by considering the V2V communication, a more effective CACC model of the ego following trucks (in a TP) (denoted as $a_n^{CACC}(t)$) which can receive an additional information of acceleration $a_{n-1}(t)$ of *preceding* CACC truck $n$-1, can be formulated in Eq. (13) (Zhang et al., 2024; Liu and Jiang, 2023; VanderWerf et al., 2001), in which $k_a$ is a control gain usually ranges from $(0,1]$ (Faber et al., 2020; Liu and Jiang, 2023).

$$a_n^{CACC}(t) = k_p\left(\Delta x_n(t) - l - s_0 - t_c v_n(t)\right) + k_d \Delta v_n(t) + k_a a_{n-1}(t) \tag{13}$$

The superiority of model (13) to (12) is discussed as follows. When the preceding CACC truck is accelerating ($a_{n-1}(t) > 0$) or decelerating ($a_{n-1}(t) < 0$), the corresponding acceleration or deceleration ($a_n^{CACC}(t)$) of the ego truck equals to the summation of the basic value given in Eq. (12) and an additional term $k_a a_{n-1}(t)$. Therefore, it is advantageous to ensure that the ego following CACC truck in a TP follows the pace of its accelerating or decelerating CACC truck leader in a string-stable manner (Faber et al., 2020). So, model (13) is adopted to control the car-following motion of the CACC following trucks in a TP, while that of the leading ACC truck is modeled using Eq. (8). Recall in Section 3.1 that, the ACC leader in a TP can transfer its kinematic parameters to its adjacent CACC follower.

### 3.3 SSM-based safety analysis approach

Aided by simulation-based vehicle trajectory data, several surrogate safety measures (SSMs) are advantageous in assessing the safety performances of the proposed mixed traffic flow. When the speed of the ego vehicle $n$ is larger than the preceding vehicle $n$-1, i.e. $v_n(t) > v_{n-1}(t)$, and assume that the speed difference between them remains constant, the

time required for a collision between the two vehicles is defined as time-to-collision (TTC) (Hayward, 1972; Oh and Kim, 2010; Jiang et al., 2023). As one of the most widely used SSMs, TTC is adopted as one of the measures for evaluating rear-end collision risks in this study, expressed in Eq. (14).

$$TTC_n(t) = \frac{x_{n-1}(t) - x_n(t) - l}{v_n(t) - v_{n-1}(t)}, \qquad \forall v_n(t) > v_{n-1}(t) \tag{14}$$

where $v_n(t)$ and $v_{n-1}(t)$ denote the speed of the two adjacent vehicles $n$-1 ahead and $n$ behind at time $t$, respectively. While $x_{n-1}(t)$ and $x_n(t)$ denote the positions of the aforementioned two adjacent vehicles at time $t$, respectively. $l$ is the length of the preceding vehicle $n$-1. However, given that the speed difference $v_n(t) - v_{n-1}(t)$ in formula (14) is assumed to be constant, TTC is time-instable when the speeds are variable. Therefore, Minderhoud and Bovy (2001) proposed two new indexes based on TTC, i.e., time-exposed TTC (TET) and time-integrated TTC (TIT), and introduced a threshold TTC* to distinguish the safe and unsafe states (Jiang et al., 2023). According to existing studies (Minderhoud and Bovy, 2001; Yao et al., 2023), TTC* generally takes values of 1.0 ~3.0 s depending on different situations.

TET is defined as the sum of time for all vehicles to approach and collide with the preceding vehicle when a TTC is lower than the threshold TTC*. The TET is given in Eq. (15)

$$TET(t) = \sum_{n=1}^{N}\sum_{t=1}^{T} \delta_t \bullet \Delta t, \quad \delta_t = \begin{cases} 1 & 0 < TTC(t) < TTC^* \\ 0 & \text{otherwise} \end{cases} \tag{15}$$

where $\delta_t$ is a binary variable, which equals 1 when the value of TTC(t) falls in the interval (0, TTC*), 0 otherwise; $\Delta t$ is the iteration time step as defined in Eq. (9); $N$ is the total number of vehicles in the simulation tests; $T$ is the total number of time steps. According to the definition of TET, the increase in TET indicates more time steps in a dangerous scenario where TTC is lower than the threshold TTC*, thus worsening the safety performance of the mixed traffic flow.

TIT is defined as the integral of the difference between TTC and TTC*. More specifically, TIT represents the change in the safety level at different TTC when it is below the threshold TTC*. An increase in TIT denotes the time exposed to TTC increases, indicating that the safety of mixed traffic flow decreases. The TIT(t) can be calculated by Eq. (16).

$$TIT(t) = \sum_{n=1}^{N}\sum_{t=1}^{T} [TTC^* - TTC(t)]\Delta t, \quad 0 < TTC(t) < TTC^* \tag{16}$$

Compared to TTC, TET and TIT focus on measuring the risk associated with the duration of dangerous driving conditions (Wang et al., 2021).

# 4 Simulation-based safety analysis

### 4.1 Experiment design

This section uses numerical simulation to investigate the safety performance of the aforementioned mixed traffic flow. As seen in Fig. 3, a hypothetical 7.0 km long, single-lane freeway with a *speed-bottleneck* section in the middle is established (Zhu et al., 2022; Yao et al., 2020). The bottleneck is 1.0 km long and extends from the beginning site of 3.0 km to 4.0 km. The flow rate is constant as $Q$ = 1400 veh/h in Sections 4.1 and 4.2. The dissipation parameter describing the stochasticity strength $\sigma$ in HDC-related SIDM in Eq. (4) is set as 0.28 (Bouadi et al., 2022). In addition, HDC penetration rates $P_{HDC}$ are set to be 0, 0.2, 0.5, then the penetration rates of HDTs ($P_{HDT}$) and TPs ($P_{TP}$) satisfy $P_{HDT} + P_{TP} = 1 - P_{HDC}$ (see Eq. (1)). TP lengths $L$, which denotes the number of trucks in a TP, are set to be 2, 3, 4, and 5 (Faber et al., 2020). The initial spatial distribution of all types of vehicles (i.e., HDC/HDT/TP) on the road stretch is assumed to follow a uniform distribution according to their mathematical relationships regarding penetration rates formulated in Eq. (2). Vehicle speeds are constrained by their maximum values $v_{max}$.

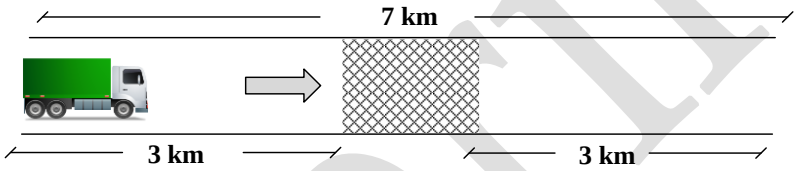


**Fig. 3** A sketch of the mixed traffic flow in the simulation experimental scenarios

On the one hand, two types of human-driven vehicles (i.e., HDCs and HDTs) are considered in the mixed traffic flow of this study. They differ in physical performance parameters in the SIDM, as shown in Table 2. On the other hand, the specific parameters of the ACC truck and CACC trucks in a TP are summarized in Table 3. The parameters in Tables 2 and 3 are dependable because they were referred to several existing studies (Shladover et al., 2018; Ramezani et al., 2018; Faber et al., 2020; Yao et al., 2020; Bouadi et al., 2022; Zhang et al., 2022, and Jiang et al., 2023). Moreover, these parameters were also approved with favorable feedback from the engineering teams of the TP program being tested on the freeways of Yangshan Deep-Water Port (Fig. 1), Shanghai, China.

Specifically, the standard values of the time headway $t_a$ of ACC leaders and that of CACC followers $t_c$ are 2.0 s and 1.2 s, respectively, referring to Shladover et al. (2018) and Zhang et al. (2022). The expected speeds of each HDC and each truck (including HDTs and TPs) are set to be 33.3 m/s (120 km/h, Jiang et al., 2023; Yao et al., 2020) and 22.2 m/s (80 km/h, Faber et al., 2020), respectively. Moreover, the square of the dissipation parameter $\sigma^2$ describing the stochasticity strengths of the HDCs and HDTs in the SIDM (see Eq. (4)) is set to be 0.28 and 0.20, respectively.

**Table 2** Parameters of the SIDM models for the HDCs and HDTs

| Parameters | Human-driven Cars | Human-driven | References |
|---|---|---|---|

| | (HDCs) | Trucks (HDTs) | |
|---|---|---|---|
| $a$ (m/s$^2$) | 1.25 | 0.4 | Faber et al. (2020) |
| $b$ (m/s$^2$) | -2.09 | -1.77 | Faber et al. (2020) |
| $T$ (s) | 1.5 | 1.5 | Faber et al. (2020) |
| $v_f$ (m/s) | 33.3 | 22.2 | Jiang et al. (2023), Faber et al. (2020) |
| $s_0$ (m) | 2.0 | 3.0 | Faber et al. (2020) |
| $l$ (m) | 4.0 | 12.0 | Faber et al. (2020) |
| $\sigma^2$ (m/s$^2$) | 0.28 | 0.20 | Bouadi et al. (2022) |

**Table 3** Parameters of the car-following model for the ACC leaders and CACC followers in a TP

| Vehicle Types | Model | Parameters (unit) | Values | References |
|---|---|---|---|---|
| ACC Truck leaders | ACC | $k_1$ (s$^{-2}$) | 0.0561 | Ramezani et al. (2018) |
| | | $k_2$ (s$^{-1}$) | 0.3393 | Ramezani et al. (2018) |
| | | $l$ (m) | 12.0 | Faber et.al. (2020) |
| | | $s_0$ (m) | 3.0 | Faber et al. (2020) |
| | | $t_a$ (s) | 2.0 | Shladover et al. (2018), Zhang et al. (2022) |
| CACC Truck followers | CACC | $k_p$ (s$^{-2}$) | 0.0074 | Ramezani et al. (2018) |
| | | $k_d$ (s$^{-1}$) | 0.0805 | Ramezani et al. (2018) |
| | | $k_a$ | 0.50 | Liu and Jiang (2023) |
| | | $l$ (m) | 12.0 | Faber et al. (2020) |
| | | $s_0$ (m) | 3.0 | Faber et.al. (2020) |
| | | $t_c$ (s) | 1.2 | Shladover et al. (2018) |

A phantom leading vehicle is deliberately placed at the leading end of the mixed traffic flow to set the simulation pace at an initial speed of 80 km/h. It gradually decelerates at a rate of -2.0 m/s$^2$ when it reaches the site of 3.0 km (i.e., the starting point of the bottleneck) until its speed reduces from 80 km/h to 10 km/h after a trip of 121.53 m (easily calculated by Newton's laws of motion, $s=\left[\left(80/3.6\right)^2-\left(10/3.6\right)^2\right]/4=121.53\ m$). The phantom vehicle travels at a constant speed of 10 km/h until it reaches the site of 4.0 km (i.e., the ending point of the bottleneck), then gradually accelerates at a rate of 2.0 m/s$^2$ until it recovers its speed to 80 km/h with a trip of another 121.53 m. The deceleration and acceleration rates of the phantom leading vehicle (i.e., ±2.0 m/s$^2$) are set within the normal scope of comfortable braking and therefore not so rapid a deceleration. The simulation duration was 20 minutes, including a 5-minute preheating time, with the simulation step being 0.1 s. Each simulation experiment was repeated five times, and the average performance metrics were output and utilized to alleviate simulation stochasticity.

### 4.2 Experimental results

*4.2.1 Trajectory data*

For simplicity and demonstrations, this section exhibits full results of vehicle trajectory under specific configurations when $P_{HDC}$ is kept as a constant of 0.2, $P_{TP}$ takes values of 0.2, 0.4, 0.6, and 0.8, and $L$ is set to be 2, 3, 4, and 5. A larger $P_{TP}$ indicates a smaller $P_{HDT}$. Therefore, $P_{TP}$ =0.8 means no HDT exists in the mixed traffic flow. It would result in a combination of sixteen (4*4) simulation scenarios. The trajectory diagrams are shown in Fig. 4 (*a*) ~ (*p*), where different colors correspond to different vehicle speeds (m/s). Note that the vehicle trajectory just presents vehicles' spatial and temporal distribution in various simulation scenarios and is not necessarily related to the safety levels.

Two main conclusions could be drawn from Fig. 4. On the one hand, for a fixed platoon length $L$ (i.e., for any row in Fig. 4), as the TP penetration rate $P_{TP}$ increases from 0.2, 0.4, 0.6 to 0.8, the dispersion of shock waves in the traffic flow gets weakened. For example, as $P_{TP}$ increases in Figs. 4 (e)~(h) when $L$ =3, it presents a more homogeneous vehicle trajectory with fewer shock waves. When $P_{TP}$ =0.8, it indicates that the human-related stochasticity derives from the fixed 20% of HDCs. In other words, a mixed flow with a higher TP penetration rate $P_{TP}$ would be less affected by the human drivers' stochasticity. On the other hand, if the shares of TPs, HDCs, and HDTs are kept constant (i.e., for any column in Fig. 4), longer TPs also result in a traffic flow with few fluctuations in spatial and temporal distribution.

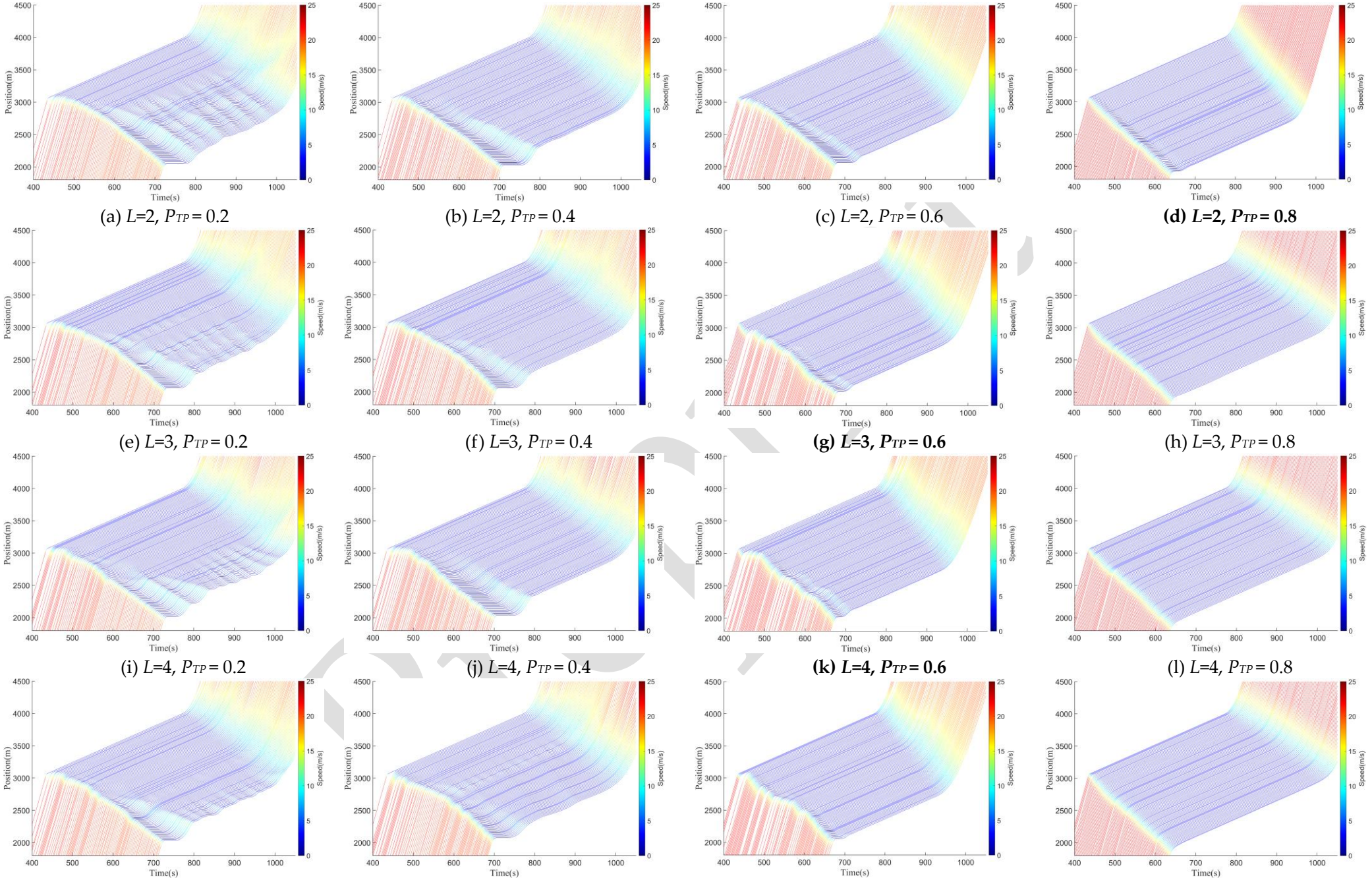


(a) $L$=2, $P_{TP}$ = 0.2 (b) $L$=2, $P_{TP}$ = 0.4 (c) $L$=2, $P_{TP}$ = 0.6 **(d) $L$=2, $P_{TP}$ = 0.8**

(e) $L$=3, $P_{TP}$ = 0.2 (f) $L$=3, $P_{TP}$ = 0.4 **(g) $L$=3, $P_{TP}$ = 0.6** (h) $L$=3, $P_{TP}$ = 0.8

(i) $L$=4, $P_{TP}$ = 0.2 (j) $L$=4, $P_{TP}$ = 0.4 **(k) $L$=4, $P_{TP}$ = 0.6** (l) $L$=4, $P_{TP}$ = 0.8

(m) $L$=5, $P_{TP}$ = 0.2 (n) $L$=5, $P_{TP}$ = 0.4 **(o) $L$=5, $P_{TP}$ = 0.6** (p) $L$=5, $P_{TP}$ = 0.8

**Fig. 4** Vehicle trajectory with a constant $P_{HDC}$=0.2, $P_{TP}$=0.2, 0.4, 0.6, 0.8, and $L$=2, 3, 4, 5

*4.2.2 Safety analysis*

In the previous section, Fig. 4 exhibited the vehicle trajectory when the share of the HDC was set to be a constant 0.2. One may wonder how the variation of the $P_{HDC}$ affects the safety levels of the mixed traffic flow. A larger $P_{HDC}$ (say 0.5) corresponds to a scenario where commuting is still vital on the freeways of the port city. Thus, $P_{HDC}$ involves three scenarios with values of 0, 0.2, and 0.5, respectively. Based on the trajectory data, the safety analysis results of the mixed traffic flow with combinatorial platooning configurations are charted in Fig. 5 (a)~(c). The horizontal coordinates denote the penetration rates of TP (HDT), i.e., $P_{TP}$ ($P_{HDT}$). The vertical coordinates are the normalized, SSM-based safety evaluation indicators $EI_{TET}$ (%) and $EI_{TIT}$ (%) after being divided by the maximum values of TET ($TET_{max}$) or TIT ($TIT_{max}$) in all three scenarios, as seen in Eqs. (17) and (18). Therefore, the three subfigures (i.e., Fig. 5 (a)~(c)) are comparable, and larger $EI_{TET}$ (%) and $EI_{TIT}$ (%) indicate a more dangerous situation.

$$EI_{TET} = TET / TET_{\max} \tag{17}$$

$$EI_{TIT} = TIT / TIT_{\max} \tag{18}$$

Moreover, $EI_{TET}$ is denoted by solid lines with dots, while $EI_{TIT}$ is represented by dashed lines with squares. Recall Eqs. (15) and (16) that the vehicle-vehicle collision risk within the mixed traffic flow increases with the values of TET and TIT. The TTC threshold (i.e., TTC*) is set as 1.5 s.

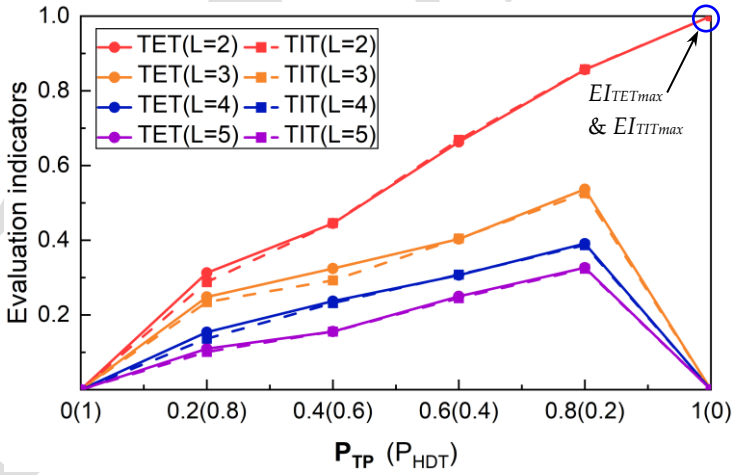


(a) $P_{HDC} = 0$

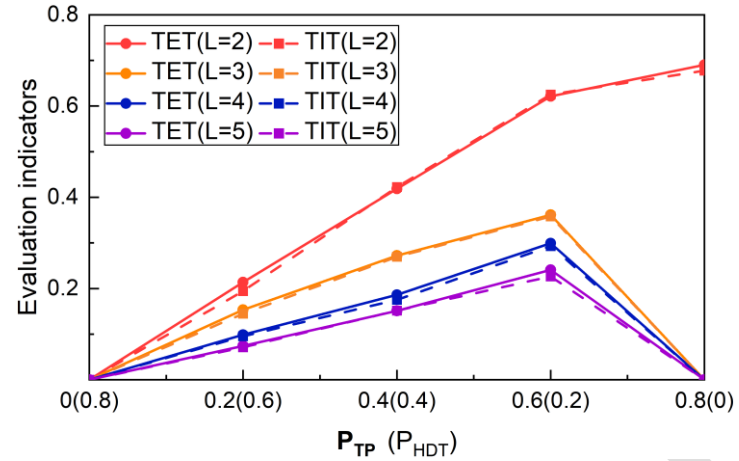


(b) $P_{HDC} = 0.2$

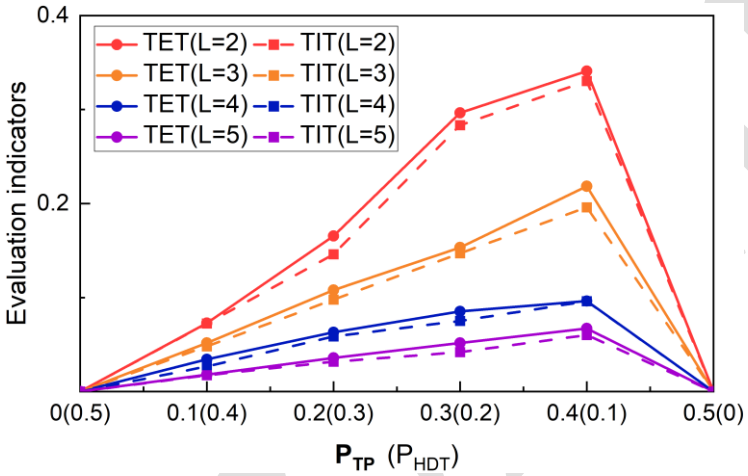


(c) $P_{HDC} = 0.5$

**Fig. 5** Safety evaluation indicators ($EI_{TET}$, $EI_{TIT}$) of the mixed traffic flow with varying $P_{HDC}$, $P_{TP}$ ($P_{HDT}$), and $L$.

Overall, with the increase of $P_{TP}$, the evolutionary trends of $EI_{TET}$ in scenarios of $P_{HDC}$ = 0, 0.2, and 0.5 are generally synchronous with those of $EI_{TIT}$, respectively. It indicates that the effects of TET in evaluating the safety performance levels of the mixed traffic flow in this study do not significantly differ from those of *TIT*. Note that the maximum values of the vertical coordinates decrease from 1.0 to 0.8 and then to 0.4 in Fig. 5 (a), (b), and (c), respectively. Therefore, one can also discriminate from Fig. 5 that the mean and extreme values of $EI_{TET}$ and $EI_{TIT}$ decrease with the HDC penetration $P_{HDC}$ (i.e., 0, 0.2, and 0.5 in sequence). This result indicates that with larger maximum deceleration rates and shorter braking distances than trucks, HDCs could improve the safety levels of mixed traffic flow. In each of Fig. 5 (a)-(c) where $P_{HDC}$, $P_{TP}$ ($P_{HDT}$) are held constants, the safety evaluation indicators $EI_{TET}$ and $EI_{TIT}$, which are negatively correlated with safety levels, decrease with the TP lengths $L$ from 2 to 5. This indicates that for a given penetration combination, longer TPs correlate with higher safety levels of mixed string flow herein. Specifically, the values of evaluation indicators with $L = 2$ (red solid and dotted lines) in Fig. 5 (a) (b) monotonously increase with $P_{TP}$ in truck-dominated scenarios ($P_{HDC}$ = 0 and 0.2). While the

trends of $L$ = 3, 4, 5 increase first and then decrease with $P_{TP}$, respectively. As shown in Fig. 5 (c), the scenario where the HDC penetration $P_{HDC}$ = 0.5 means the ratio of HDCs to trucks is 1:1, and the evaluation indicators' values demonstrate a trend of increasing and then decreasing with the increase of $P_{TP}$. It implies that the safety of mixed traffic flow in this scenario decreased and then improved with $P_{TP}$, which is consistent with the results of the study by Yao et al. (2020). The inflection points in Fig. 5 (c) occur at $P_{TP}$ = 0.3 for the lengths of TP $L$ being 3, 4, and 5, respectively. These results indicate that for a given configuration of penetration rates (i.e., Eq. (1)), there would be the worst safety state related to the lengths of TP $L$=3, 4, 5.

### 4.3 Sensitivity analysis

This section will investigate the impacts of different variables on the safety performance levels of the mixed traffic flow proposed in this study. It is a tremendous computational burden to conduct an all-sided sensitivity analysis to test the effects of all parameters on the results. Therefore, a more efficient way is to conduct selected sensitivity analyses for specific, important parameters. The parameters considered herein include different traffic flow rates, headway combinations, different vehicle types of the TP leader, and different stochasticity strengths.

#### *4.3.1 Impacts of different traffic flow rates*

The results of the safety evaluation indicators $EI_{TET}$ (%) and $EI_{TIT}$ (%) under various traffic flow rates $Q$ =1200/1400/1600/1800 *veh/h* in the scenario of $P_{HDC}$ = 0.2 are illustrated in Figs. 6 and 7, respectively. In Fig. 6, the values of $EI_{TET}$ increase with the traffic flow rate $Q$ when other conditions (i.e., $P_{TP}$ and $L$) are equal. This indicates that the safety levels of the saturated mixed traffic flow worsen with the increase of total traffic flow rate $Q$. It can also be found from Fig. 6 that for a congested traffic scenario (i.e., Q=1800 veh/h), both the increase of the TP penetration rate $P_{TP}$ can exacerbate the safety levels of the mixed traffic flow with a given platoon length $L$, which is consistent with results found in Faber et al., (2020).

Comparing Fig. 6 with Fig. 7, it can be found that other conditions being equal (TP penetration rate $P_{TP}$, traffic flow rate Q), the values of $EI_{TET}$ and $EI_{TIT}$ of the mixed traffic flow decrease with the platoon length $L$. This result reaches a consensus that an increase of $L$ would raise the safety levels of the given mixed traffic flow in this study. As shown in Fig. 6 (a) and Fig. 7 (a), when $L$ = 2 and $Q$ = 1200 *veh/h*, the $EI_{TET}$ and $EI_{TIT}$ of the mixed traffic flow exhibit a trend of increase and then decrease with the rise of $P_{TP}$ (from 0.2 to 0.8). In contrast, this fluctuant trend spreads to the case of $Q$ = 1400 *veh/h* when $L$ = 3 (Fig. 6 (b) and Fig. 7 (b)) and $L$ = 4 (Fig. 6 (c) and Fig. 7 (c)). Finally, when $L$ = 5 (Fig. 6 (d) and Fig. 7 (d)), this *first-increase-then-decrease* trend spreads further to $Q$=1600 *veh/h*. This indicates that high penetrations of TPs with a longer $L$ would improve the safety levels of the more saturated,

mixed traffic flow. This also hints that a longer TP is advantageous and would potentially lower the collision risk levels in congested conditions on port freeways in peak shipping seasons.

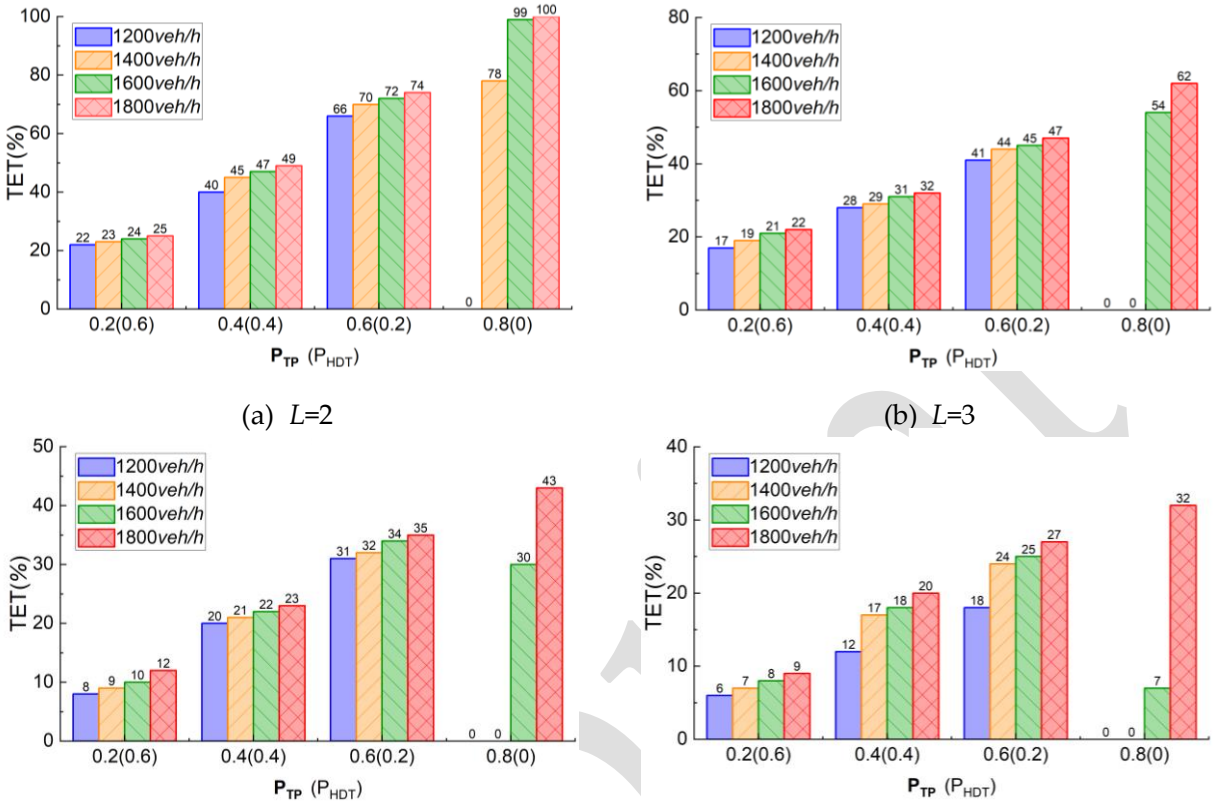


**Fig. 6** $EI_{TET}$ values for different flow rates $Q$ (1200/1400/1600/1800 *veh/h*), platoon lengths $L$ (2, 3, 4, 5), and penetration combinations $P_{TP}$ ($P_{HDT}$)

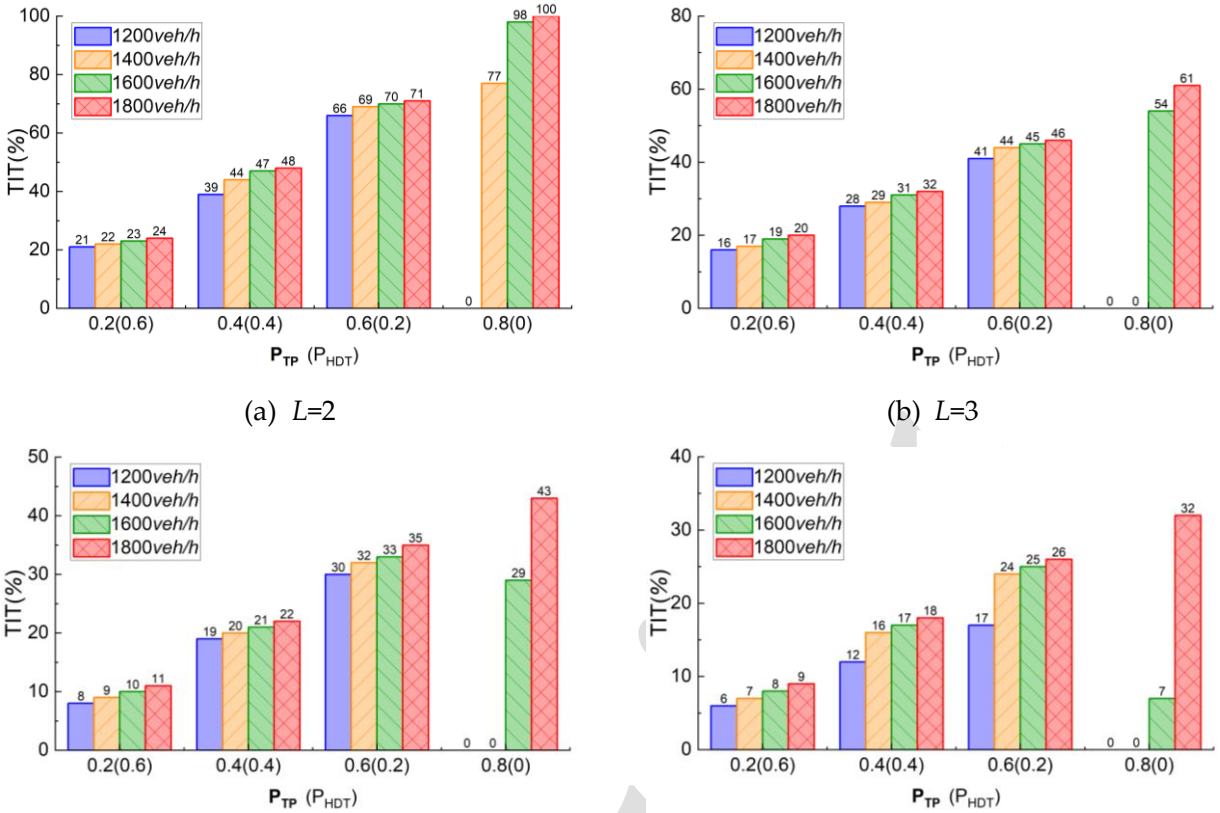


(a) *L*=2 (b) *L*=3

(c) *L*=4 (d) *L*=5

**Fig. 7** $EI_{TIT}$ values for different combinations of flow rates *Q* (1200/1400/1600/1800 *veh/h*), platoon lengths *L* (2, 3, 4, 5), and penetration $P_{TP}$ ($P_{HDT}$)

*4.3.2 Impacts of different headway combinations ($t_a$ and $t_c$)*

Time headway is a vital index depicting the vehicle-vehicle dynamics. Another interesting issue is how the combinations of various time headways affect the safety performance of the mixed traffic flow. The mixtures of expected headways in this section refer to those of ACC platoon truck leaders $t_a$ taken as 1.5 s, 2.0 s, 2.5 s, 3.0 s, and those of the CACC truck followers $t_c$ taken as 0.6 s, 0.9 s, 1.2 s, 1.5 s, 1.8 s, respectively. To inquire into the optimal combinations of headways (i.e., $t_a$ and $t_c$) in the TP-involved mixed traffic flow, this section hypothesizes a simulation scenario with *Q* =1800 *veh/h*, $P_{HDC}$ = 0.2, $P_{TP}$ = 0.2, 0.4, 0.6, and *L* = 2, 3, 4, 5, respectively. The results in Fig. 8 describe the $EI_{TET}$ values for different headway combinations ($t_a$ and $t_c$) in twelve scenarios.

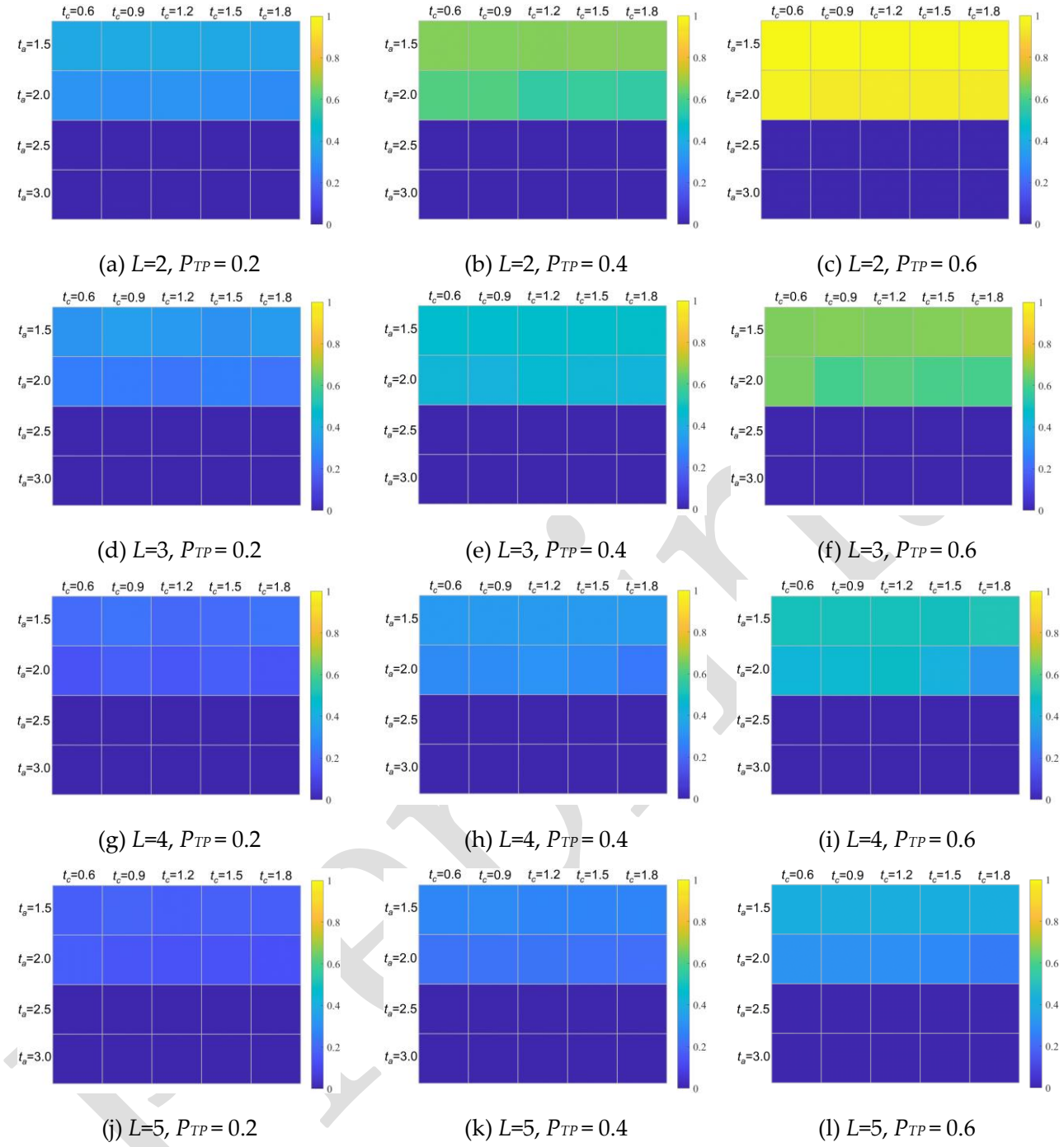


(a) $L$=2, $P_{TP}$ = 0.2 (b) $L$=2, $P_{TP}$ = 0.4 (c) $L$=2, $P_{TP}$ = 0.6

(d) $L$=3, $P_{TP}$ = 0.2 (e) $L$=3, $P_{TP}$ = 0.4 (f) $L$=3, $P_{TP}$ = 0.6

(g) $L$=4, $P_{TP}$ = 0.2 (h) $L$=4, $P_{TP}$ = 0.4 (i) $L$=4, $P_{TP}$ = 0.6

(j) $L$=5, $P_{TP}$ = 0.2 (k) $L$=5, $P_{TP}$ = 0.4 (l) $L$=5, $P_{TP}$ = 0.6

**Fig. 8** $EI_{TET}$ for selected scenes with different combinations of headways $t_a$ and $t_c$

As shown in Fig. 8, when the headway of ACC truck leader $t_a$ holds constant (i.e., for each row in each subfigure), the increase of $t_c$ (0.6s, 0.9s, 1.2s, 1.5s, 1.8s) do not significantly affect the $EI_{TET}$ values of the mixed traffic flow. This indicates that for a given $t_a$, the safety performance levels are not highly correlated with the headways of CACC truck followers $t_c$ in a TP. Compared with $t_a$=2.5 s, 3.0 s, shorter $t_a$ (1.5 s, 2.0 s) worsens the safety levels of the mixed flow. Moreover, as shown in Fig. 8 (c), for a shorter $t_a$ (i.e., 1.5 s, 2.0 s), a mixed flow with more TPs (i.e., a higher $P_{TP}$, say 0.6) and a shorter TP length $L$ (say 2) will result in more ACC truck leaders (see $N_{AT}$ in Eq. (2)), and gradually intensifies this deterioration effect.

By contrast, when the CACC intra-platoon headway $t_c$ holds constant (i.e., for each

column in each subfigure), the $EI_{TET}$ values decrease significantly but not linearly with the increase of $t_a$ (i.e., 1.5 s, 2.0 s, 2.5 s, 3.0 s). It indicates that for a given $t_c$, a larger headway of ACC truck leaders $t_a$ is advantageous to improve the safety levels of the mixed traffic flow because of a larger safe distance ahead of the leading truck in a TP. This effect presents a sharp drop when the transition occurs from $t_a$ =2.0 s to 2.5 s, indicating that a threshold between 2.0 and 2.5 evenly divides the impact of $t_a$ on the safety levels of the mixed traffic flow into two sections. In each section, the values of $EI_{TET}$ when $t_a$ = 2.5 s and 3.0 s do not differ much from each other.

The results of $EI_{TIT}$ are analogous to those of $EI_{TET}$, so omitted for simplification.

As a result, it is advised to prefer various headway ($t_a$ and $t_c$) combinations for safer traffic flow when: (1) time headways for ACC truck leaders $t_a$ are set to be equal to or higher than 2.5 s; (2) given that CACC technique can furnish the essential communication supports among CACC trucks, the time headway for CACC followers $t_c$ (0.6 s ~1.8 s) could be properly small, which also be beneficial to safety, and a larger roadway capacity as well.

### *4.3.3 Impacts of different vehicle types of a TP leader (CACC, HDT vs ACC)*

At the initial stage of applying the TPs, an important and interesting issue is to investigate the effects of different vehicle types (say, an HDT or an ACC truck) of TP leaders on the safety levels of the mixed traffic flow considered in this study. In Fig. 1, the TPs involved in the previous experiments are assumed to comprise degraded ACC truck leaders and CACC-based truck followers. As shown in Fig. 9, this section will relax the assumption of the ACC leader in a TP to a broader types of TP leaders, i.e., an HDT (Fig. 9 (a)) or a CACC truck (Fig. 9 (b)). The configurations of the model parameters for an HDT leader and a CACC leader here follow their original settings adopted in Tables 2 and 3 in Section 4.1 as a free truck and a CACC follower, respectively.

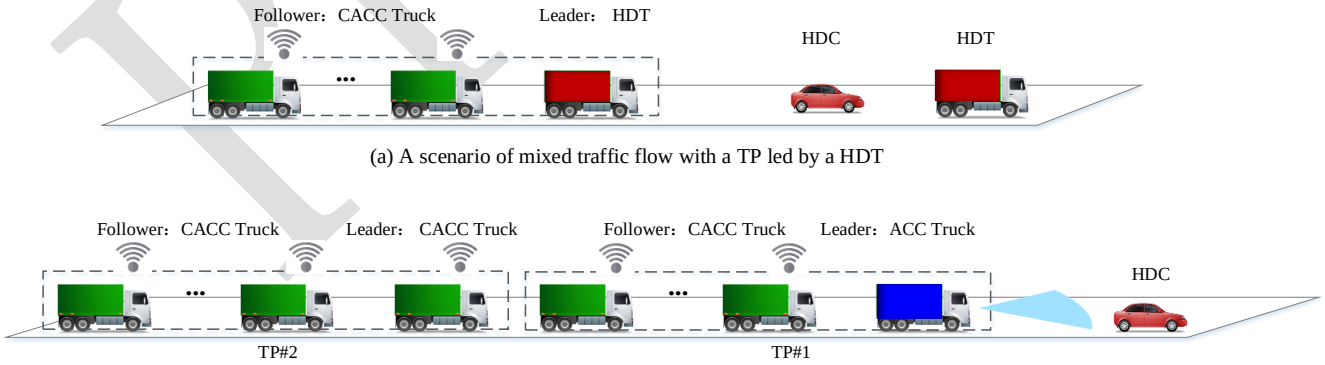


(a) A scenario of mixed traffic flow with a TP led by a HDT

(b) A scenario of mixed traffic flow with the TP-TP Communication

**Fig. 9** Example of platooning schemes with different types of TP leaders (i.e., HDTs, CACC/ACC trucks)

In this section, the traffic flow rate $Q$ is also set to be 1800 *veh/h*, and the penetration rates of HDCs $P_{HDC}$ and TPs $P_{TP}$ are set to be 0.2 and 0.2 (initial development stage), 0.4 (medium development stage), 0.6 (high-level development stage), respectively. The

resulting impacts of different types of TP leaders (i.e., ACC, CACC, and HDT) on the safety performance levels (i.e., $EI_{TET}$ and $EI_{TIT}$) of the mixed traffic flow are tabulated in Tables 4 and 5, respectively.

**Table 4** $EI_{TET}$ (%) for different platoon leaders (ACC/CACC/HDT) in the mixed traffic flow ($P_{HDC}$=0.2)

| $L$ | $P_{TP}$ ($P_{HDT}$) | | | | | | | | |
|---|---|---|---|---|---|---|---|---|---|
| | **0.2** (0.6) | | | **0.4** (0.4) | | | **0.6** (0.2) | | |
| | ACC | CACC | HDT | ACC | CACC | HDT | ACC | CACC | HDT |
| 2 | 34 | 31 | 0 | 67 | 49 | 0 | 100 | 63 | 0 |
| 3 | 25 | 23 | 0 | 44 | 37 | 0 | 58 | 44 | 0 |
| 4 | 19 | 17 | 0 | 30 | 26 | 0 | 48 | 38 | 0 |
| 5 | 13 | 12 | 0 | 24 | 22 | 0 | 36 | 33 | 0 |

**Table 5** $EI_{TIT}$ (%) for different platoon leaders (ACC/CACC/HDT) in the mixed traffic flow ($P_{HDC}$=0.2)

| $L$ | $P_{TP}$ ($P_{HDT}$) | | | | | | | | |
|---|---|---|---|---|---|---|---|---|---|
| | **0.2** (0.6) | | | **0.4** (0.4) | | | **0.6** (0.2) | | |
| | ACC | CACC | HDT | ACC | CACC | HDT | ACC | CACC | HDT |
| 2 | 33 | 32 | 0 | 68 | 48 | 0 | 100 | 62 | 0 |
| 3 | 23 | 21 | 0 | 43 | 35 | 0 | 57 | 43 | 0 |
| 4 | 18 | 17 | 0 | 28 | 23 | 0 | 47 | 37 | 0 |
| 5 | 13 | 12 | 0 | 24 | 22 | 0 | 36 | 32 | 0 |

The results demonstrate that when $P_{TP}$ and $L$ are held constant, the $EI_{TET}$ and $EI_{TIT}$ of the mixed traffic flow decrease when an ACC truck leader is changed to a CACC leader and then to an HDT. This suggests that compared to a TP led by an ACC truck, both a CACC truck leader (which can communicate between two adjacent TPs) and an HDT leader in TPs can improve the safety performance levels of the mixed traffic flow in various degrees. A TP led with an HDT would have a higher potential for safety improvement. In addition, we found that when the TP leaders are altered from an ACC truck to a CACC one, the decreasing rates of $EI_{TET}$ and $EI_{TIT}$ in mixed traffic flow increase with the TP proportion $P_{TP}$ but drop with platoon length $L$. This implies that for higher penetration rates of the TPs in the mixed flow, changing the TP leader from an ACC truck to a CACC would increase the safety of the mixed flow, while the marginal effects of lengthening the TP on improving the safety levels fade away. Accordingly, compared with ACC leaders, CACC leaders have a more pronounced impact on improving the safety levels at the high-level development stage (with a higher $P_{TP}$) and shorter platoon lengths.

*4.3.4 Impacts of different stochasticity strengths on the safety performance level*

This section will discuss the effects of the dissipation parameter $\sigma$ in Eq. (4), describing the stochasticity strength of human-driven vehicles on the safety levels of the mixed traffic flow. For clarity, the values of dissipation parameters $\sigma$ for HDCs and HDTs

are selected twice as those in Table 2 hereafter, respectively. And the traffic flow rate $Q$ is set to be 1400 veh/h in this section, and the penetration rates of HDCs $P_{HDC}$ and TPs $P_{TP}$ are set to be 0.2, and 0.2, 0.4, 0.6, 0.8, respectively. We proposed the percentage change (PC) PC of TET ($PC_{TET}$) is formulated in Eq. (18), while the PC of TIT ($PC_{TIT}$) is formally comparable:

$$PC_{TET} = \frac{TET_{\sigma_{2x}} - TET_{\sigma_{1x}}}{TET_{\sigma_{1x}}} \times 100\% \quad (18)$$

where $\sigma_{1x}$ indicates the stochasticity strength adopted in preceding HDC/HDT SIDMs (i.e., 0.28 and 0.20 respectively in Table 2), while $\sigma_{2x}$ means the stochasticity strengths to be twice as large as $\sigma_{1x}$. The impacts of different stochasticity strengths on the safety performance levels (i.e., note they are TET and TIT here) of the mixed traffic flow are shown in Fig. 10 (a) and (b). Note that the overall trend and appearance of the two subfigures are highly alike. $PC$>0 indicates that the safety levels of the mixed traffic flow deteriorate as the stochasticity strengths double.

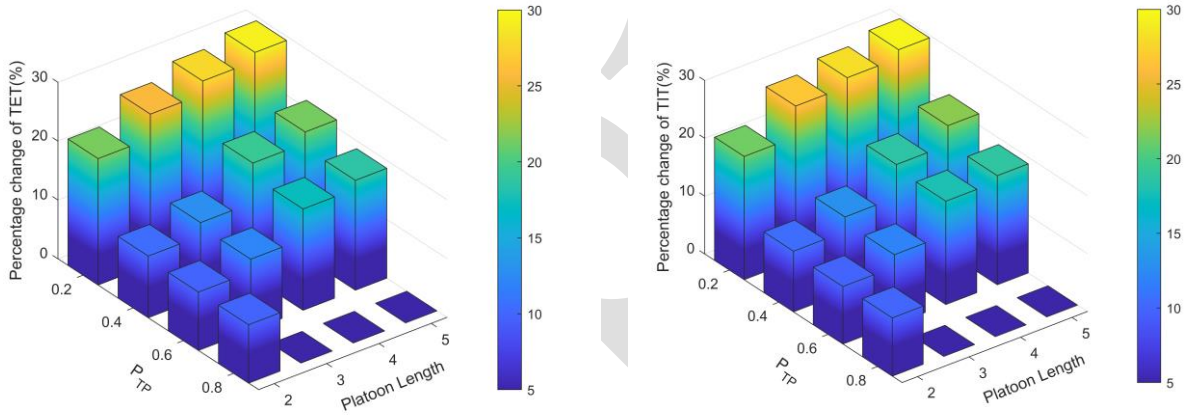


(a) Percentage change of TET (b) Percentage change of TIT

**Fig. 10** The PC of TET and TIT under two levels of stochasticity strengths

The empirical findings reveal that with a double in stochasticity strength $\sigma$, both TET and TIT exhibit an upward trend in the context of mixed traffic flow. This denotes a decrease in the safety levels of mixed traffic flow with an augmentation in the stochastic nature of HDVs. Under the condition of a constant TP length $L$, the increase of $P_{TP}$ is correlated with a mitigated rate of change in TET and TIT for mixed traffic flow. Simultaneously, it is discerned that, for a given $P_{TP}$, a larger $L$ corresponds to an increasing PC in both TET and TIT for the mixed traffic flow. This suggests that, compared to shorter TPs, stochasticity would make longer ones more impressionable. In other words, longer TPs, while displaying enhanced traffic flow coordination, also manifest a greater susceptibility to the effects of stochasticity introduced by human drivers.

# 5 Conclusions and future directions

This study considered a novel complex traffic flow, a mixture of human-driven and intelligence-driven vehicles and passenger and freight transport. Precisely, the mixed traffic flow consists of scheduled truck platoons equipped with (cooperative) adaptive cruise control (TPs-(C)ACC) and traditional human-driven vehicles, including (passenger) cars (HDCs) and (freight) container trucks (HDTs). Car-following frameworks, including SIDM, ACC, and CACC models, were utilized for systematic numerical, SSM-based simulation experiments. The following conclusions can be drawn:

As the TP penetration rate $P_{TP}$ increases, the oscillation of the mixed traffic flow considered in this study gets weakened (see Fig. 4). Other things being equal, longer TPs contribute to a safer mixed flow. Under given conditions, more HDCs can benefit the operation safety levels of the mixed traffic flow considered in this study (Fig. 5). Other things being equal, the safety levels of the mixed traffic flow deteriorate with the increase of total traffic flow rate (Figs. 6 and 7). For a given CACC intra-platoon headway, larger headways of ACC truck leaders are advantageous to improving the safety levels of the mixed traffic flow (Fig. 8). For TPs with shorter $t_a$ (1.5 s 2.0 s), higher penetrations of TPs with a shorter platoon length would worsen the safety levels of the mixed traffic flow (Fig. 8). For a given combination of penetration rates ($P_{TP}$, $P_{HDT}$, $P_{HDC}$), the marginal effects of lengthening the TPs on improving the safety levels of mixed traffic flow wear off (Tables 4 and 5). For a given $P_{TP}$, a mixed flow with longer TPs would be more impressionable by the stochastic behavior of human drivers. (Fig. 10).

This study conducted an initial step to understand the complexities of the novel traffic flow and provides a theoretical foundation for the operation and development of TPs. However, several promising areas require future investigations. Theoretically, more efforts would be expected in analyzing the stochastic differential equations formulating the relationship among car-following stochasticity, stability, and safety of the mixed traffic flow proposed in this study (Bouadi et al., 2022). Secondly, this study only considered the scheduled platooning of TPs, and the impact of real-time and opportunistic platooning on the safety of the mixed traffic flow remains unknown. Moreover, to make the scenarios more realistic and applicable to actual systems like ports or logistics, future studies could extend the basic single-lane scenario to a multi-lane freeway one. This would allow for considering more complex driving behaviors such as lane-changing, braking, overtaking, and platooning regrouping. Finally, in addition to TTC, TET, and TIT adopted in the current study, it is promising if more alternative SSMs, such as Deceleration Rate to Avoid the Crash (DRAC, Cooper and Ferguson, 1976; Wang et al., 2021), rear-end collision risk index (RCRI, Oh et al., 2006), etc., could be applied to evaluate the safety of the mixed traffic flow in analogous obstacle situations**.** In summary, investigating the impacts of various characteristic combinations on the safety of the mixed traffic flow in more complex situations is challenging but of great significance.

# Declaration of Competing Interest

The authors declare that they have no known competing financial interests or personal relationships that could have appeared to influence the work reported in this paper.

# Acknowledgment

This study was supported by the Shanghai Science and Technology Commission [grant numbers 23692107100], the National Government-sponsored Postdoctoral Program by China Scholarship Council [grant number 202008310074], the Shuguang Program of the Shanghai Education Development Foundation and Shanghai Municipal Education Commission [grant number 22SG46], the Natural Science Foundation of Shanghai [grant number 22ZR1426600], the Innovation Program of Shanghai Municipal Education Commission [grant number 2023SKZD16], and the Foundation for Jiangsu Key Laboratory of Traffic and Transportation Security [grant number TTS2021-06].

## Appendix. List of abbreviations

Table A. List of main Abbreviations.

| Abbreviations | Full name |
|---|---|
| ACC | adaptive cruise control |
| CACC | cooperative adaptive cruise control |
| CAVs | connected and automated vehicles |
| HDCs | human-driven cars |
| HDTs | human-driven trucks |
| HDVs | human-driven vehicles |
| IDM | intelligent driver model |
| PC | percentage change |
| SIDM | stochastic intelligent driver model |
| SSMs | surrogate safety measures |
| TET | time-exposed TTC |
| TIT | time-integrated TTC |
| TPs-(C)ACC | truck platoons with (cooperative) adaptive cruise control |
| TP | truck platoon |
| TTC | time-to-collision |
| V2V | vehicle to vehicle |

# References

Alam, A., Besselink, B., Turri, V., MåRtensson, J., Johansson, K.H., 2015. Heavy-Duty Vehicle Platooning for Sustainable Freight Transportation: A Cooperative Method to Enhance Safety and Efficiency. *IEEE Control Syst. Mag.* 35 6, 34–56.

Axelsson, J. 2016. Safety in vehicle platooning: A systematic literature review. *IEEE Transactions on Intelligent Transportation Systems*, 18(5), 1033-1045.

Bai, J., Lee, J., Mao, S. 2024. Effects of Adaptive Cruise Control System on Traffic Flow and Safety Considering

Various Combinations of Front Truck and Rear Passenger Car Situations. *Transp. Res. Rec. J. Transp. Res. Board*, 03611981231223982.

Binder, K., Heermann, D., Binder, K. 1992. Monte Carlo simulation in statistical physics (Vol. 8). Berlin: Springer-Verlag.

Brooks, S., Gelman, A., Jones, G., Meng, X. 2011. Handbook of Markov Chain Monte Carlo. CRC press.

Bouadi, M., Jia, B., Jiang, R., Li, X., Gao, Z. Y. 2022. Stochastic factors and string stability of traffic flow: Analytical investigation and numerical study based on car-following models. *Transp. Res. Part B Methodol.*, 165, 96-122.

Bouadi, M., Jiang, R., Jia, B., Zheng, S. T. 2024. String Stability Analysis of Cooperative Adaptive Cruise Control Vehicles Considering Multi-Anticipation and Communication Delay. *IEEE Trans. Intell. Transp. Syst.*

Bhoopalam, A.K., Agatz, N., Zuidwijk, R., 2018. Planning of truck platoons: A literature review and directions for future research. *Transp. Res. Part B Methodol.*, 107, 212–228.

Calvert, S.C., Schakel, W.J., van Arem, B., 2019. Evaluation and modelling of the traffic flow effects of truck platooning. *Transp. Res. Part C Emerg. Technol.*, 105, 1–22.

Chen, D., Ahn, S., Chitturi, M., Noyce, D., 2018. Truck platooning on uphill grades under cooperative adaptive cruise control (CACC). *Transp. Res. Part C Emerg. Technol.*, 94, 50–66.

Dai, Y., Wang, C., Xie, Y., 2023. Explicitly incorporating surrogate safety measures into connected and automated vehicle longitudinal control objectives for enhancing platoon safety. *Accid. Anal. Prev*. 183, 106975.

Deng, Q., 2016. A General Simulation Framework for Modeling and Analysis of Heavy-Duty Vehicle Platooning. *IEEE Trans. Intell. Transp. Syst.* 17 11, 3252–3262.

Faber, T., Sharma, S., Snelder, M., Klunder, G., Tavasszy, L., van Lint, H., 2020. Evaluating Traffic Efficiency and Safety by Varying Truck Platoon Characteristics in a Critical Traffic Situation. *Transp. Res. Rec. J. Transp. Res. Board* 2674 10, 525–547.

Graham, C., Talay, D. 2013. Stochastic simulation and Monte Carlo methods: mathematical foundations of stochastic simulation (Vol. 68). Springer Science & Business Media.

Hayward J. C., 1972. Near-miss determination through use of a scale of danger, *Highw. Res. Rec.*, 384

Jiang, C., Bhat, C. R., Lam, W. H. 2020. A bibliometric overview of Transportation Research Part B: Methodological in the past forty years (1979–2019). *Transp. Res. Part B*, 138, 268-291.

Jiang, C., He, J., Zhu, S., Zhang, W., Li, G., Xu, W. 2023. Injury-Based Surrogate Resilience Measure: Assessing the Post-Crash Traffic Resilience of the Urban Roadway Tunnels. *Sustainability*, 15(8), 6615.

Jiang, C., Lu, L., Chen, S., Lu, J. J. 2016. Hit-and-run crashes in urban river-crossing road tunnels. *Accident Analysis & Prevention*, 95, 373-380.

Jiang, C., Tay, R., Lu, L. 2021. A skewed logistic model of two-unit bicycle-vehicle hit-and-run crashes. *Traffic injury prevention*, 22(2), 158-161.

Jiang, R., Hu, M., Zhang, H., Gao, Z., Jia, B., Wu, Q., 2015. On some experimental features of car-following behavior and how to model them. *Transp. Res. Part B Methodol.* 80, 338–354.

Jiang, R., Jin, C., Zhang, H., Huang, Y., Tian, J., Wang, W., Hu, M., Wang, H., Jia, B., 2018. Experimental and empirical investigations of traffic flow instability. *Transp. Res. Part C* 94, 83–98.

Jiang, R., Wu, Q., Zhu, Z., 2001. Full velocity difference model for a car-following theory. *Phys. Rev. E*, 64(1), 017101.

Jiang, Y., Ren, T., Ma, Y., Wu, Y., Yao, Z. 2023. Traffic safety evaluation of mixed traffic flow considering the maximum platoon size of connected automated vehicles. *Phys. A Stat. Mech. Its Appl.*; 612 128452.

Jo, Y., Kim, J., Oh, C., Kim, I., Lee, G. 2019. Benefits of travel time savings by truck platooning in Korean freeway networks. *Transport Policy*, 83, 37-45.

Kalos, M., Whitlock, P., 2009. Monte Carlo methods. John Wiley & Sons.

Lammert, M.P., Duran, A., Diez, J., Burton, K., Nicholson, A., 2014. Effect of Platooning on Fuel Consumption of Class 8 Vehicles Over a Range of Speeds, Following Distances, and Mass. *SAE Int. J. Commer. Veh*. 7 2, 626–639.

Lee, Y., Ahn, T., Lee, C., Kim, S., Park, K., 2020. A Novel Path Planning Algorithm for Truck Platooning Using V2V Communication. *Sensors* 20 24, 7022.

Li, T., Chen, D., Zhou, H., Laval, J., Xie, Y. 2021. Car-following behavior characteristics of adaptive cruise control vehicles based on empirical experiments. *Transp. Res. Part B Methodol.*, 147, 67-91.

Li, Y., Li, Z., Wang, H., Wang, W., Xing, L., 2017a. Evaluating the safety impact of adaptive cruise control in traffic oscillations on freeways. *Accid. Anal. Prev*. 104, 137–145.

Li, Y., Wang, H., Wang, W., Xing, L., Liu, S., Wei, X., 2017b. Evaluation of the impacts of cooperative adaptive cruise control on reducing rear-end collision risks on freeways. *Accid. Anal. Prev.* 98, 87–95. doi:10.1016/j.aap.2016.09.015

Lioris, J., Pedarsani, R., Tascikaraoglu, F.Y., Varaiya, P., 2017. Platoons of connected vehicles can double throughput in urban roads. *Transp. Res. Part C Emerg. Technol.*, 77, 292–305.

Liu, H., Jiang, R. 2023. Efficient control of connected and automated vehicles on a two-lane highway with a moving bottleneck. *Chinese Physics B*, 32(5), 054501.

Lyu, H., Wang, T., Cheng, R., Ge, H. 2022. Improved longitudinal control strategy for connected and automated truck platoon against cyberattacks. *IET Intelligent Transport Systems*, 16(12), 1710-1725.

Ma, Y., Liu, Q., Fu, J., Liufu, K., Li, Q. 2023. Collision-avoidance lane change control method for enhancing safety for connected vehicle platoon in mixed traffic environment. *Accid. Anal. Prev*. 184, 106999.

Mahdinia, I., Arvin, R., Khattak, A. J., Ghiasi, A. 2020. Safety, energy, and emissions impacts of adaptive cruise control and cooperative adaptive cruise control. *Transp. Res. Rec. J. Transp. Res. Board*, 2674(6), 253-267.

Milanés V, Shladover S. 2014. Modeling cooperative and autonomous adaptive cruise control dynamic responses using experimental data. Transportation Research Part C: Emerging Technologies. 48:285-300.

Minderhoud, M.M., Bovy, P.H.L., 2001. Extended time-to-collision measures for road traffic safety assessment. *Accid. Anal. Prev.* 331, 89–97.

Ngoduy, D., Lee, S., Treiber, M., Keyvan-Ekbatani, M., Vu, H., 2019. Langevin method for a continuous stochastic car-following model and its stability conditions. *Transp. Res. Part C Emerg. Technol.*, 105, 599–610.

Nowakowski, C., Thompson, D., Shladover, S.E., Kailas, A., Lu, X.-Y., 2016. Operational Concepts for Truck Maneuvers with Cooperative Adaptive Cruise Control. *Transp. Res. Rec. J. Transp. Res. Board* 2559 1, 57–64. doi:10.3141/2559-07

Oh, C., Kim, T., 2010. Estimation of rear-end crash potential using vehicle trajectory data. *Accid. Anal. Prev.* 42 6, 1888–1893.

Oh, C., Park, S., Ritchie, S.G., 2006. A method for identifying rear-end collision risks using inductive loop detectors. *Accid. Anal. Prev.* 38, 295–301

Pi, D., Xue, P., Wang, W., Xie, B., Wang, H., Wang, X., Yin, G. 2023. Automotive platoon energy-saving: A review. *Renewable and Sustainable Energy Reviews*, 179, 113268.

Protter, P. 2005. Stochastic differential equations. Springer Berlin Heidelberg.

Ramezani, H., Shladover, S.E., Lu, X.-Y., Altan, O.D., 2018. Micro-simulation of Truck Platooning with Cooperative Adaptive Cruise Control: Model Development and a Case Study. *Transp. Res. Rec. J. Transp. Res. Board* 2672 19, 55–65.

Rubinstein, R., Kroese, D., 2016. Simulation and the Monte Carlo method. John Wiley & Sons.

Shladover, S., Lu, X., Yang, S., Ramezani, H., Spring, J., Nowakowski, C., Nelson, D., 2018. Cooperative Adaptive Cruise Control (CACC) For Partially Automated Truck Platooning: Final Report. Federal Highway Administration–Exploratory Advanced Research Program

Shladover, S.E., Nowakowski, C., Lu, X.-Y., Ferlis, R., 2015. Cooperative Adaptive Cruise Control: Definitions

and Operating Concepts. *Transp. Res. Rec. J. Transp. Res. Board* 2489 1, 145–152.

Schneider, J., Kirkpatrick, S. 2007. Stochastic optimization. Springer Science & Business Media.

Tian, J., Zhang, H., Treiber, M., Jiang, R., Gao, Z.-Y., Jia, B., 2019. On the role of speed adaptation and spacing indifference in traffic instability: Evidence from car-following experiments and its stochastic model. *Transp. Res. B Methodol.* 129, 334–350.

Treiber, M., Hennecke, A., Helbing, D., 2000. Congested traffic states in empirical observations and microscopic simulations. *Phys. Rev. E* 62 2, 1805–1824.

Tu, Y., Wang, W., Li, Y., Xu, C., Xu, T., Li, X., 2019. Longitudinal safety impacts of cooperative adaptive cruise control vehicle's degradation. *J. Safety Res.* 69, 177–192.

VanderWerf, J., Shladover, S., Kourjanskaia, N., Miller, M., Krishnan, H. 2001. Modeling effects of driver control assistance systems on traffic. *Transp. Res. Rec*., 1748(1), 167-174.

van Arem, B., van Driel, C.J.G., Visser, R., 2006. The Impact of Cooperative Adaptive Cruise Control on Traffic-Flow Characteristics. *IEEE Trans. Intell. Transp. Syst.* 7 4, 429–436.

van Nunen, E., Esposto, F., Saberi, A.K., Paardekooper, J.-P., 2017. Evaluation of safety indicators for truck platooning. Presented at the *2017 IEEE Intelligent Vehicles Symposium (IV), IEEE, Los Angeles, CA, USA*, pp. 1013–1018.

Wang, Y., Li, X., Tian, J., Jiang, R., 2020. Stability analysis of stochastic linear car-following models. *Transp. Sci.* 54, 274–297.

Wang, C., Xie, Y., Huang, H., Liu, P., 2021. A review of surrogate safety measures and their applications in connected and automated vehicles safety modeling. *Accid. Anal. Prev.* 157, 106157.

Wang, M., van Maarseveen, S., Happee, R., Tool, O., van Arem, B., 2019. Benefits and Risks of Truck Platooning on Freeway Operations Near Entrance Ramp. *Transp. Res. Rec. J. Transp. Res. Board* 2673 8, 588–602.

Xing, Y., Lu, J., Lu, L., Jiang, C., Cai, X. 2014. Comprehensive safety assessment model of road long tunnel based on VISSIM. *Intelligent Automation & Soft Computing*, 20(4), 501-514.

Xu, T., Laval, J.A., 2019. Analysis of a two-regime stochastic car-following model: Explaining capacity drop and oscillation instabilities. *Transp. Res. Rec.* 2673, 610–619.

Yang, D., Kuijpers, A., Dane, G., der Sande, T. van, 2019. Impacts of large-scale truck platooning on Dutch highways. Transp. Res. Procedia, 21st EURO Working Group on Transportation Meeting, EWGT 2018, 17th – 19th September 2018, Braunschweig, Germany 37, 425–432.

Yao, Z., Hu, R., Jiang, Y., Xu, T., 2020. Stability and safety evaluation of mixed traffic flow with connected automated vehicles on expressways. *J. Safety Res.* 75, 262–274.

Yao, Z., Hu, R., Wang, Y., Jiang, Y., Ran, B., Chen, Y., 2019. Stability analysis and the fundamental diagram for mixed connected automated and human-driven vehicles. *Phys. Stat. Mech. Its Appl.* 533, 121931.

Yao, Z., Wang, Y., Liu, B., Zhao, B., Jiang, Y., 2021. Fuel consumption and transportation emissions evaluation of mixed traffic flow with connected automated vehicles and human-driven vehicles on expressway. *Energy* 230, 120766.

Yao Z., Gu Q., Jiang Y., Ran B. 2022. Fundamental diagram and stability of mixed traffic flow considering platoon size and intensity of connected automated vehicles. *Phys. Stat. Mech. Its Appl.* 604.

Yao, Z., Wu, Y., Wang, Y., Zhao, B., Jiang, Y. 2023. Analysis of the impact of maximum platoon size of CAVs on mixed traffic flow: An analytical and simulation method. *Transp. Res. Part C Emerg. Technol.*, 147, 103989.

Yu, H., Jiang, R., He, Z., Zheng, Z., Li, L., Liu, R., Chen, X., 2021. Automated vehicle-involved traffic flow studies: A survey of assumptions, models, speculations, and perspectives. *Transp. Res. Part C Emerg. Technol*. 127, 103101.

Zhang, J., Wu, K., Cheng, M., Yang, M., Cheng, Y., Li, S., 2020. Safety Evaluation for Connected and Autonomous Vehicles' Exclusive Lanes Considering Penetrate Ratios and Impact of Trucks Using Surrogate Safety Measures. *J. Adv. Transp*. 2020, 1–16.

Zhang, P., Zhu, H., Zhou, Y., 2022. Modeling cooperative driving strategies of automated vehicles considering trucks' behavior. *Phys. Stat. Mech. Its Appl.* 11.

Zhang, Tianya Terry, Peter J. Jin, Sean T. McQuade, Alexandre M. Bayen, Benedetto Piccoli. 2023. Car-Following Models: A Multidisciplinary Review. arXiv:2304.07143v4

Zhu, L., Lu, L., Wang, X., Jiang, C., Ye, N., 2022. Operational Characteristics of Mixed-Autonomy Traffic Flow on the Freeway with On- and Off-Ramps and Weaving Sections: An RL-Based Approach. *IEEE Trans. Intell. Transp. Syst*. 23 8, 13512–13525.